Fractals, Vol. 30, No. 3 (2022) 2250040 (11 pages)

DOI: 10.1142/S0218348X22500402

World Scientific
www.worldscientific.com

UNIVERSAL MULTIFRACTAL STATIONARY DENSITIES IN EXPANDING PIECEWISE LINEAR COUPLED MAPS

DEEPAK JALLA* and KIRAN M. KOLWANKAR†,‡
*K. J. Somaiya College of Science and Commerce
Mumbai, Maharashtra 400077, India
†Department of Physics, Ramniranjan Jhunjhunwala College
Ghatkopar West, Mumbai 400086, India
‡kiran.kolwankar@gmail.com

Received April 23, 2021
Accepted November 18, 2021
Published March 24, 2022

Abstract

The phenomenon of synchronization in coupled chaotic maps has been studied extensively by the researchers in nonlinear dynamics for several years. But, there is hardly any study of the stationary densities of coupled maps as a function of the coupling parameter. Here, we numerically analyze stationary densities of two nonlinearly coupled tent maps. In the process, we find that the emergent stationary density can become multifractal even if the stationary density of the individual maps is smooth. In this work, we study piecewise linear and everywhere expanding maps as the stationary density for these maps is described by a simple functional relation. By extensive numerical simulations we find that for this class of maps the multifractal spectrum is universal and does not seem to change with the coupling or map parameters. The existence of this multifractal nature is not surprising, *a posteriori*, as it is known the densities satisfying similar functional relation are known to be multifractal but the form of the multifractal spectrum here is intriguing as it does not seem to conform to the existing theory of multifractal functions.

Keywords: Multifractals; Coupled Chaotic Maps; Synchronization; Universality.

‡Corresponding author.

1. INTRODUCTION

Studying coupled nonlinear systems has immense importance owing to wide ranging applications and phenomena including synchronization.[1] As a result, coupled nonlinear systems have been an active area of research for more than 30 years. Coupling of nonlinear systems can introduce additional twists leading to a more complex phase space. Nevertheless, there exists an invariant measure or a stationary density which allows statistical characterization of the irregular dynamics of the system. Therefore, it is natural to study the stationary densities of coupled systems as a function of the coupling parameter. However, not much understanding has been obtained on the effect of coupling on the stationary density and, in turn, its use in studying synchronization, except for the following two papers. In Ref. 2, the multifractal characteristic of the coupled *lattice* of Hénon maps was studied for a small range of coupling parameters wherein the individual map is known to have fractal characteristics and, in Ref. 3, the invariant measure of a chain of coupled maps was studied but not its multifractal nature. Keeping this in mind we analyze the stationary density of simple coupled systems, their multifractal nature and their dependence on the coupling parameter.

The fractal dimension[4–7] provides a tool to capture the irregularity of a set, here the graph of a function, arising as a result of a nonlinear process. It is also well known that at times the dimension can be insufficient to characterize the irregularity completely and a spectrum of dimensions, called the multifractal spectrum, might be needed. The multifractal spectrum, at least in some cases, gives the dimension of a set on which we have a given Hölder exponent which is defined as follows: the Hölder exponent of a function $\rho(x)$ at x_0 is defined as the largest value of h, where $0 < h < 1$ (it is possible to extend the definition beyond this range), such that

$$|\rho(x) - \rho(x_0)| \leq C|x - x_0|^h$$

for some constant C. According to this definition, a discontinuity in a function corresponds to the Hölder exponent equal to zero and for a smooth function it is one everywhere.

The celebrated example of the multifractal function is, of course, the velocity field of a turbulent fluid. Frisch and Parisi[8] developed the structure function formalism to obtain the multifractal spectrum of a function. Since then, the multifractal approach has become standard in several fields.[9,10] The essence of the method of Frisch and Parisi was to assume the following scaling:

$$S(\delta, q) = \int |\rho(x + \delta) - \rho(x)|^q dx \sim \delta^{\zeta(q)}, \quad (1)$$

for small δ, and then obtain the singularity spectrum $D(h)$ by Legendre transformation of $\zeta(q)$. Here, $D(h)$ reflects the dimension of the set of points where the Hölder exponent of the function is h (this is equivalent to the function $f(\alpha)$ used in the multifractal formalism for measures). This way of obtaining the singularity spectrum is known as the structure function approach to the multifractal formalism.

Detecting the multifractality in experimental or numerical data has been a challenge. Though the structure function method was a good theoretical approach, it was limited as a computational tool. To overcome this difficulty, a method using wavelet transforms was developed and successively modified for better performance. The essential idea was to use the wavelet coefficients $C(a, b)$, where a is the scale and b is the position, in the integral above and define $S(a, q)$ as follows:

$$S(a, q) = \int |C(a, b)|^q db. \quad (2)$$

With the assumption that $S(a, q) \sim a^{\zeta(q)}$, the singularity spectrum is obtained by taking the Legendre transform of $\zeta(q)$. Muzy *et al.*[11,12] refined this method further. The new method, called the wavelet transform modulus maxima (WTMM), defines the partition function $S(a, q)$ as

$$S(a, q) = \sum_l \sup_{(b=l(a))} |C(a, b)|^q, \quad (3)$$

where l is a local maxima line of the wavelet transform and the sum is taken over this discrete set of maxima lines. This method has been used extensively in various applications.[11–13]

Later, a new method using wavelet leaders[14,15] was been proposed which was shown to be more efficient than WTMM. The method of calculating the multifractal spectra using wavelet leaders[14,15] has the same basic structure as the WTMM method.[13] There is one key difference in how the partition functions are calculated. Instead of using the local maxima of the modulus of the continuous wavelet transform in WTMM, wavelet leaders use discrete wavelet transforms (DWTs) and calculate the partition function by finding the leader of the wavelet transform. If $c(a, x)$ is a wavelet coefficient then the wavelet leader $L(a, x)$ is its maximum in a region around x over all scales smaller than a. For DWT, $a = 2^j$ and

$x = 2^j k$). Now, if $S(a, q)$ gives the qth order moment of wavelet leaders then we have $S(a, q) \sim a^{\zeta(q)}$ and the dimension $D(h)$ is given by the Legendre transform of $\zeta(q)$. Wavelet leaders have been used in various applications.[16]

On the other hand, mathematicians have developed an extensive multifractal formalism for a class of measures, or more generally functions, satisfying certain conditions[17–20] in which a direct formula for the dimension spectrum can be written down from the parameters of the transformations. Using this formula the multifractal spectrum is constructed. For example, Jaffard[19] defined a class of functions called self-similar functions which are solutions of a functional equation of the type

$$F(x) = \sum_i \lambda_i F(S_i^{-1}(x)) + g(x), \tag{4}$$

where S_is are compositions of an isometry with the mapping $x \to \mu_i x$ with $|\mu_i| < 1$. Several conditions are needed on the transformations S_is and the function $g(x)$. The important one being that the S_is satisfy the open set condition (OSC). That is, there exists a bounded open set Ω such that $S_i(\Omega) \subset \Omega$ and $S_i(\Omega) \cap S_j(\Omega) = \emptyset$ if $i \neq j$. Also, it is assumed that the μ_is scale by the same factor in all directions in higher dimensions. Then it was shown that the dimension spectrum can be obtained in terms of the λ_is and μ_is. In particular the smallest value of the Hölder exponent is given by $h_{\min} = \inf \frac{\log \lambda_i}{\log \mu_i}$ and the largest value of the Hölder exponent is given by $h_{\max} = \sup \frac{\log \lambda_i}{\log \mu_i}$.

2. MULTIFRACTAL NATURE OF THE STATIONARY DENSITIES

Our system consists of a nonlinear map $f(x)$ which is a function from $[0, 1]$ to $[0, 1]$. We consider two such identical maps coupled to each other as follows:

$$\begin{aligned} x_{n+1} &= (1 - \epsilon) f(x_n) + \epsilon f(y_n), \\ y_{n+1} &= \epsilon f(x_n) + (1 - \epsilon) f(y_n), \end{aligned} \tag{5}$$

where ϵ is the coupling parameter. If we write $X = (x, y)^T$, a two-dimensional column vector, then the above set of equations defines a transformation T such that

$$X_{n+1} = T(X_n). \tag{6}$$

We obtain the stationary density by starting from a uniform distribution over the whole of phase space Ω and letting this density evolve according to the dynamics. We discard first 1000 iterations. In order to have better statistics, here we restrict ourselves to the cross-section of this stationary density along the synchronization manifold, that is, the line $x = y$. This amounts to then counting the instances when the trajectory lies in a strip of size 2δ around the line $x = y$. We have chosen $\delta = 2^{-8}$ throughout after verifying that doubling the size does not change the results much.

In order to rule out any effect of the finiteness of the floating point representation we have carried out our simulations using an infinite precision arithmetic as provided by a type bigfloat in Julia[21] implemented using MPFR libraries. We have taken care to choose the number of bits in the floating point representation twice as that of the number of map operations on any initial condition (the number of map operations on any initial condition was less than 5000 and the number of bits in the floating point representation was chosen as 10,000). It has also been verified that our results remain the same by choosing the number of bits larger than this.

The stationary densities of several of the standard maps, like the logistic map at $\mu = 4$, the tent map or the skewed tent map are known to be uniform or a simple smooth function (except at a few points). Here, we observe that as soon as two copies of any of these maps are coupled nonlinearly, even with a very small coupling parameter, we obtain a very complex invariant density. Figure 1 depicts the cross-sections of the stationary densities along the synchronization manifold for four different choices of coupled identical maps.

In the case of the logistic map ($\mu = 4$), it is known that the invariant density has square root singularities at $x = 0$ and $x = 1$ and is smooth for all other intermediate values of x but for the coupled logistic maps (both with $\mu = 4$) the stationary density is irregular throughout the interval. One can notice that the singularities are spread throughout the interval. The stationary density of the tent map is uniform but after coupling two tent maps it too becomes very irregular. In fact, its fractal nature was first pointed out in Ref. 22. One can also notice some discontinuities in the density. These singularities arise because of the discontinuity of the initial distribution at the boundaries. In Ref. 23, the support of this invariant measure was used to carry out a global analysis of synchronization. One can understand the origin of these discontinuities from the analysis carried out there. Similar observations are valid for the asymmetric tent map and the bit shift map.

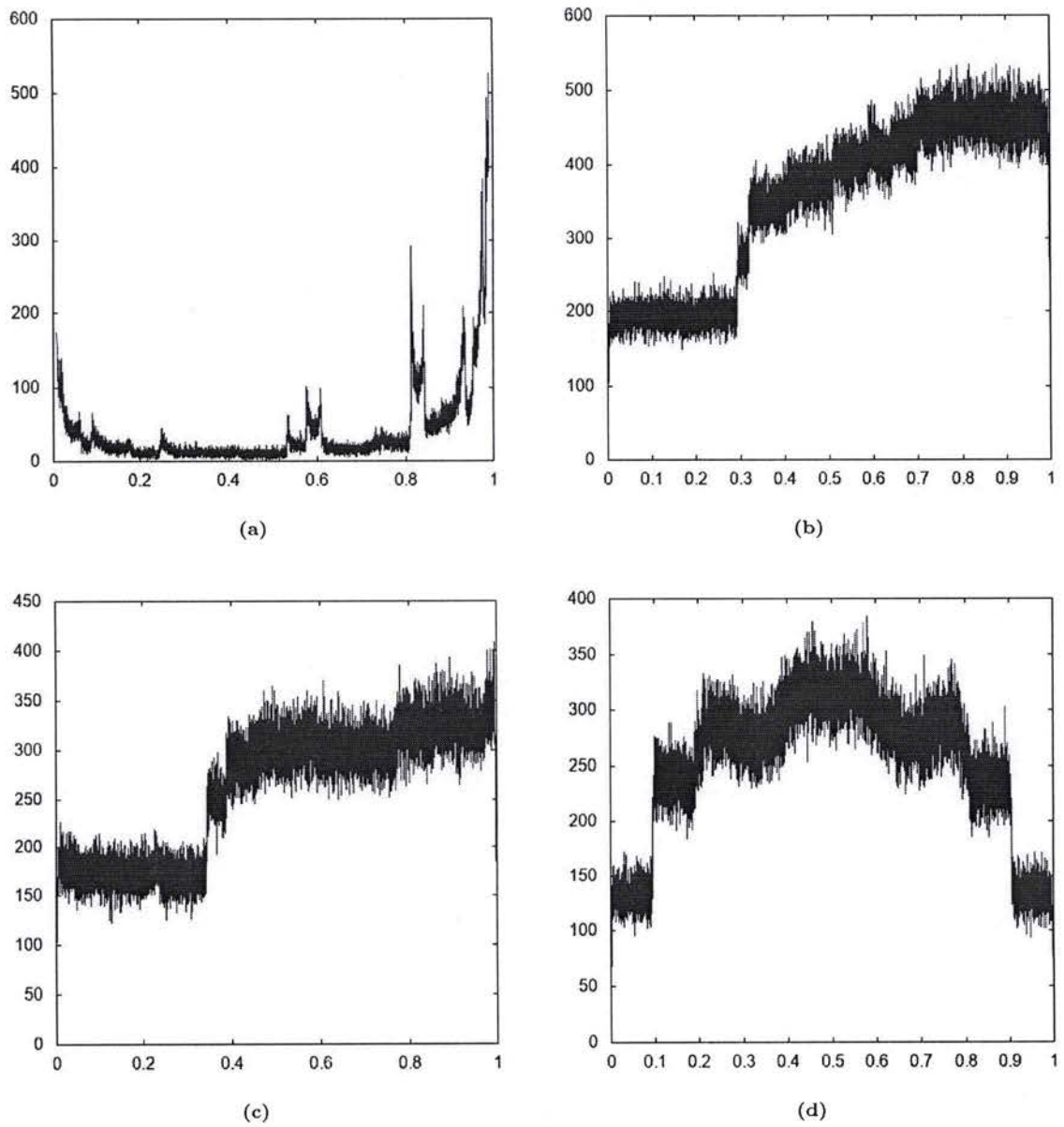

Fig. 1 Examples of the stationary densities of coupled systems on synchronization manifold **(a)** logistic map with $\mu = 4$, **(b)** symmetric tent map, **(c)** asymmetric tent map with $a = 0.1$ and **(d)** bit shift map. $\epsilon = 0.08$, there are 4×10^6 points on the synchronization manifold and 12,000 bins.

We carried out a multifractal analysis of these stationary densities restricted to the synchronization manifold. It should be emphasized that it was the stationary density treated as a function that was analyzed and not its integrated measure. We first used the WTMM method but it turned out to be inadequate for these highly self-affine graphs of the functions. Then we used the newly developed method using wavelet leaders.

2.1. Results

We first consider the symmetric tent map defined by

$$f(x) = \begin{cases} 2x & 0 \leq x < 1/2, \\ 2 - 2x & 1/2 \leq x < 1, \end{cases}$$

with two of them coupled as described in Eq. (5).

Figure 2 shows the results of the multifractal analysis of the stationary density of this map for

$\epsilon = 0.1$ using the wavelet leaders method. In Fig. 2a, we show a log–log plot of $S(a, q)$ versus a for different values of q. The power law scaling is clearly visible. Then in Fig. 2b, we show the ζ_q which are given by the slopes of the straight line fits in Fig. 2a. The dimension spectra, obtained as the Legendre transform of ζ_q, are plotted in Fig. 2c for different choices of the total number of points. Figure 2d depicts the spectra for different sizes of the bins. The convergence is clearly visible. In order to further confirm the multifractal nature of the spectra, we have estimated the error bars in two different ways as depicted in Figs. 2e and 2f. In the first method, we took 12 different data sets of the

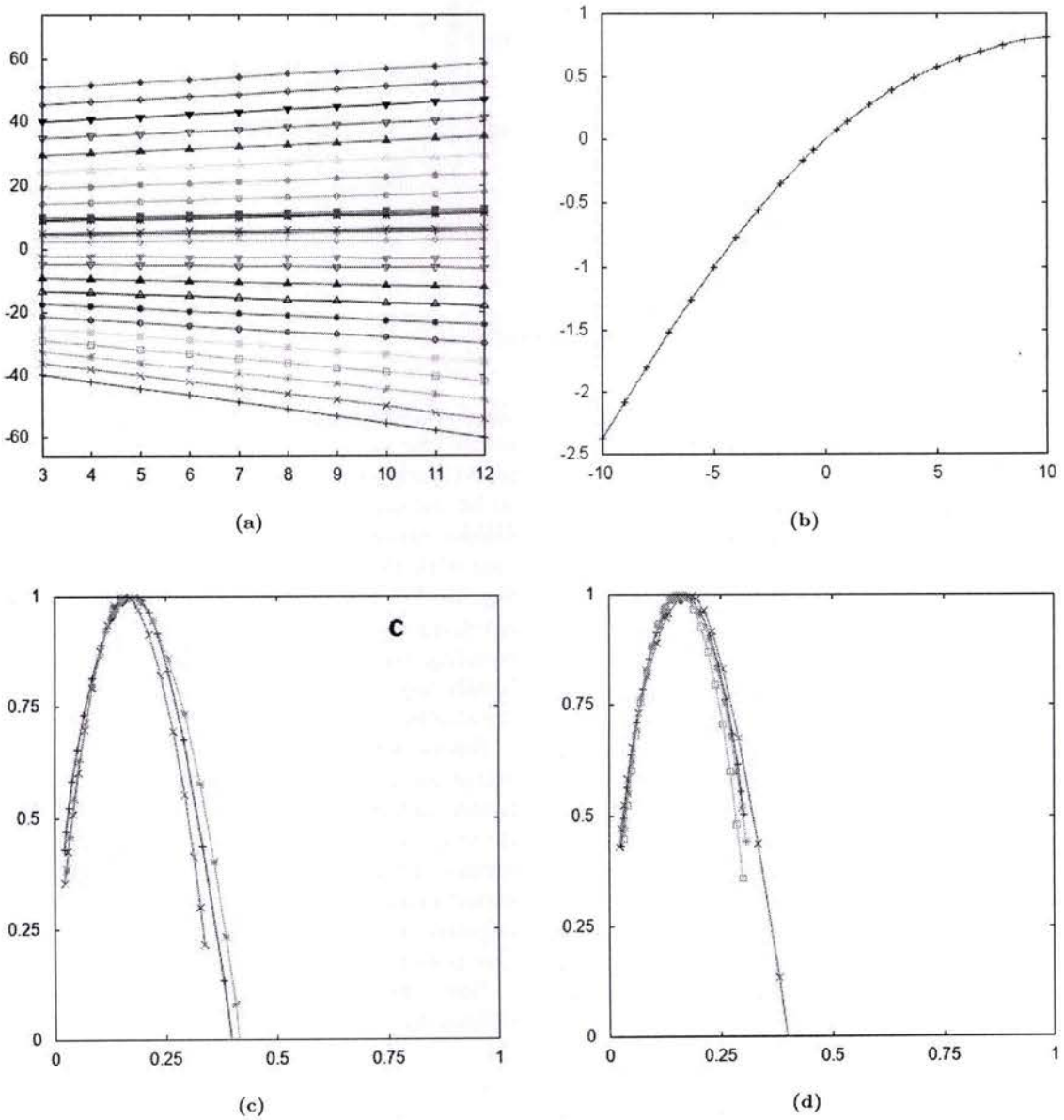

Fig. 2 The multifractal spectrum for the coupled tent maps with $\epsilon = 0.08$. **(a)** $S(a, q)$ versus a plotted for different values of q (-10 to $+10$), **(b)** $\zeta(q)$ versus q, **(c)** the dimension spectrum for different values of N, the number of points on the synchronization manifold but the same number of bins (=4000) ($+ -4 \times 10^5$, $\times -8 \times 10^5$, $* -1.2 \times 10^6$). **(d)** The dimension spectrum for different number of bins ($+ -2000$, $\times -4000$, $* -8000$ and $\square -16{,}000$) with 1.2×10^6 number of points on the synchronization manifold. **(e)** The error bars estimated using standard deviation over 12 different spectra by using 12 different data of 1×10^6 points and 12,000 bins. **(f)** Confidence intervals generated by non-parametric bootstrap procedure as implemented in the wavelet leader toolbox.[14] This is a clear numerical evidence that the spectra are multifractal.

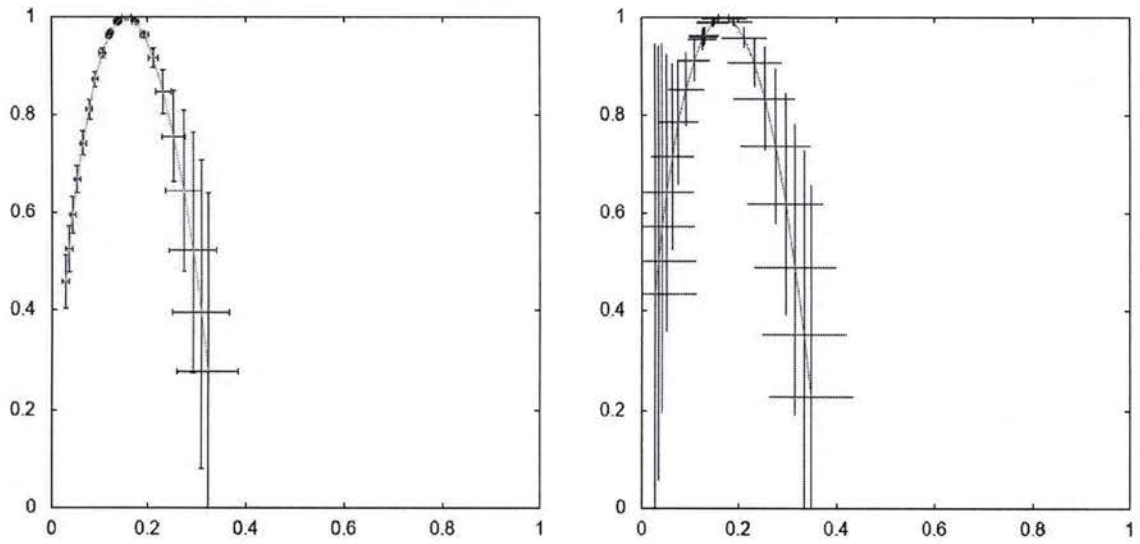

(e) (f)

Fig. 2 (*Continued*)

same size (10^6 points) and thus generated 12 different spectra with 12,000 bins. Figure 2e shows the error bars estimated from the standard deviations of h values and corresponding $D(h)$ values. Figure 2f shows the confidence intervals generated by the non-parametric bootstrap procedure provided by the wavelet leader toolbox.[14] This is convincing numerical evidence that the spectra are indeed multifractal.

In order to ascertain the role of statistical fluctuations, we analyzed the stationary density by making the coupling constant zero. In this case, we had pure statistical fluctuations in our data. When we carried out the multifractal analysis of this data we did not find power law scaling for $S(a, q)$. When further steps are carried out by fitting a straight line to whatever log–log plot of $S(a, q)$ and a was obtained, it resulted in a spectrum consisting of a cluster of points. This cluster of points seemed to approach the point $(0, 1)$. Hence one could conclude that no multifractal spectrum was observed when the coupling was zero. This implies that the multifractal spectrum that we observed originated purely from the dynamics that the coupling between the maps had introduced.

As we have observed above, we expect the stationary density of the coupled tent map to have discontinuities at a countable number of points. As explained below, the discontinuity in a function corresponds to a Hölder exponent equal to zero and the countable set of points has dimension zero. As a result, one would expect the dimension spectrum to pass through the point $(0, 0)$ which, we note, seems to be the case. It can also be seen that there is no Hölder exponent greater than 0.5 which is consistent with the very irregular nature of the graph in Fig. 1b. What is more surprising is the fact that the spectrum seems to be very robust with changing the coupling parameter. As shown in Fig. 3a, there is hardly any change in the spectrum as the coupling parameter ϵ is varied.

Before we proceed, we would like to bring to attention a related fact. As has been pointed out before, in the case of stationary density of the logistic map (Fig. 1a), there are stronger singularities spread throughout the interval. As a result, one expects that the spectrum would cross over to the negative side and not pass through the point $(0, 0)$. Our preliminary analysis indeed confirms this.

Now, we consider the asymmetric tent map defined by

$$f_a(x) = \begin{cases} \dfrac{x}{a}, & 0 \le x < a, \\ \dfrac{1-x}{1-a}, & a \le x < 1, \end{cases}$$

where a is the skew-factor. It is known that though a single skewed tent map is chaotic it has uniform invariant measure.[24] In light of this, it is surprising that as soon as we introduce small coupling

(here $\epsilon = 0.08$) the resultant stationary density is multifractal as is shown in Figs. 3c and 3d. Figure 3c depicts the spectra for different values the skewness parameter a and a fixed value of the coupling constant ϵ and Fig. 3d shows the spectra for a fixed value of a and different values of ϵ. As one notices, the spectra are robust in this case too.

Our next choice of the map is the symmetric bit shift map which is also called the Bernoulli map. It

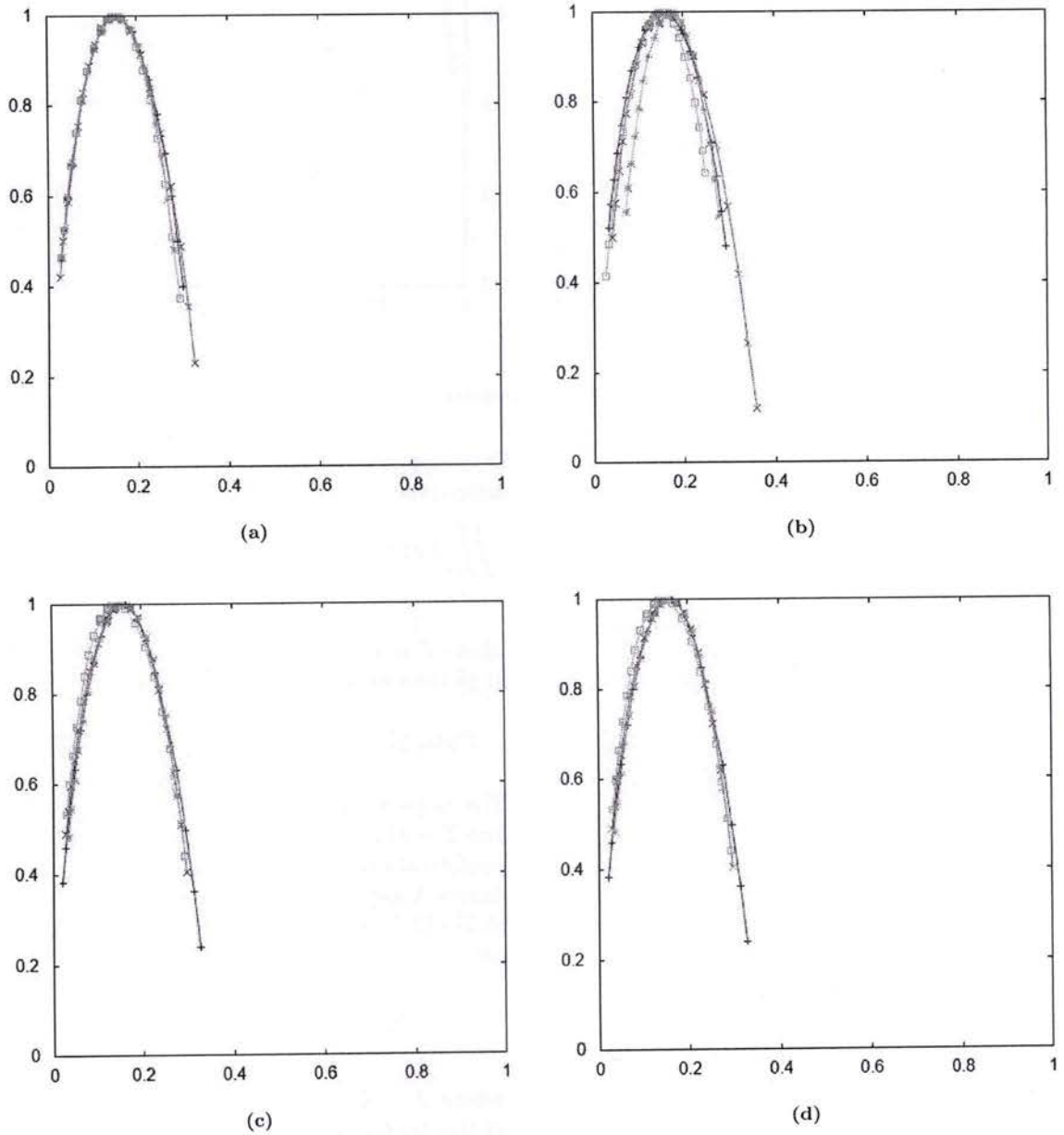

Fig. 3 The multifractal spectra for **(a)** the symmetric tent map with varying ϵ (+ -0.08, × -0.12, ∗ -0.16, □ -0.20), **(b)** the bit shift maps for different coupling constants ϵ (+ -0.08, × -0.12, ∗ -0.16, □ -0.20), **(c)** the asymmetric tent map with different skewness parameter (+ -0.1, × -0.2, ∗ -0.3, □ -0.4) and fixed coupling constant $\epsilon = 0.08$, **(d)** the asymmetric tent map with different coupling constants ϵ (+ -0.08, × -0.12, ∗ -0.16, □ -0.20) and fixed skewness parameter $a = 0.4$, **(e)** the asymmetric bit shift map for fixed asymmetry ($\Delta = 0.06$) and different couplings ϵ (+ -0.08, × -0.12, ∗ -0.16, □ -0.20), **(f)** the asymmetric bit shift map for the same coupling ($\epsilon = 0.08$) and different skewness parameter Δ (+ -0.04, × -0.06, ∗ -0.08 and □ -0.10). The number of bins used in all these sub-figures is 12,000 and the number of points on the synchronization manifold are $>10^7$.

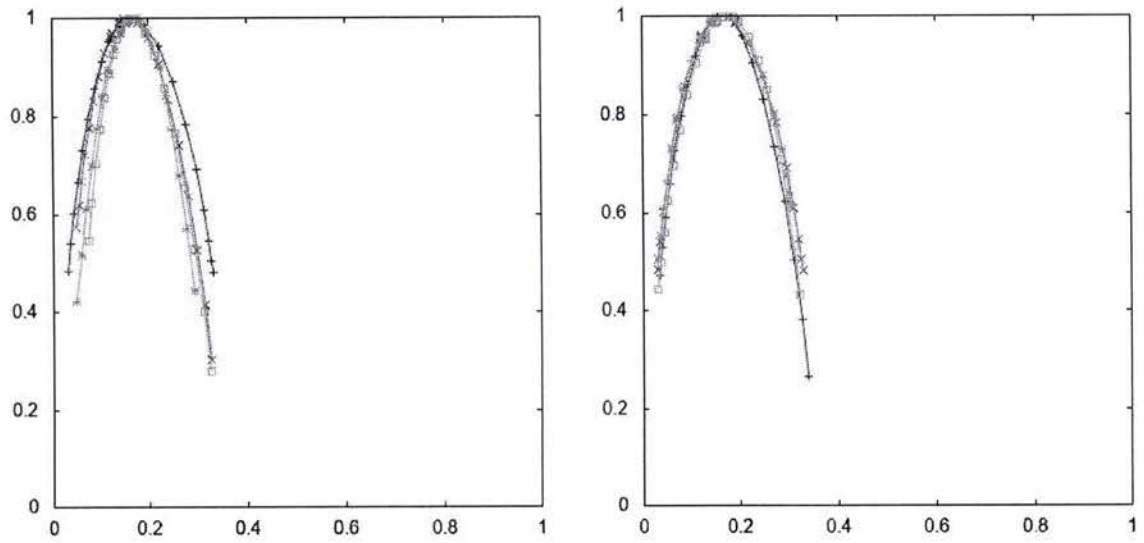

(e) (f)

Fig. 3 (*Continued*)

is defined by

$$f(x) = \begin{cases} 2x, & 0 \le x < 1/2, \\ 2x - 1, & 1/2 \le x < 1. \end{cases}$$

This map too shows multifractal character in the stationary density when coupled (Fig. 3b). Even in this case there is no variation in the spectra as the coupling parameter is varied.

Now, we introduce an asymmetry[25] in this map and consider the skewed bit shift map defined by

$$f(x) = \begin{cases} \dfrac{x}{0.5 - \Delta}, & 0 \le x < 0.5 - \Delta, \\ \dfrac{x}{0.5 + \Delta} - \dfrac{0.5 - \Delta}{0.5 + \Delta}, & 0.5 - \Delta < x \le 1, \end{cases}$$

where Δ is a parameter characterizing the asymmetry. The stationary density of this map too has multifractal nature when two of them are coupled together. This is shown in Figs. 3e and 3f. In this case too the spectra do not change on varying ϵ (Fig. 3e) nor with varying the skewness parameter Δ (Fig. 3f).

3. MATHEMATICAL ANALYSIS

It is necessary to understand these findings through a mathematical analysis of these measures. The invariant measure can be calculated by using the Frobenius–Perron operator $P : L^1 \to L^{126}$ which is defined as

$$\iint_D P\rho(x', y')dx'dy' = \iint_{T^{-1}(D)} \rho(x', y')dx'dy', \tag{7}$$

where T is as in Eq. (6). If we choose $D = [0, x] \times [0, y]$ then we get

$$P\rho(x, y) = \frac{\partial}{\partial x}\frac{\partial}{\partial y}\iint_{T^{-1}(D)} \rho(x', y')dx'dy'. \tag{8}$$

The maps we have chosen are not invertible, therefore T is also not invertible. For all the maps under consideration, T consists of four disjoint parts. We denote them by T_i^{-1}, $i = 1, \ldots, 4$. If $X \in \Omega = [0, 1] \times [0, 1]$, since f is not in general symmetric, we get

$$P\rho(X) = \sum_{i=1}^{4} J_i^{-1}(X)\rho(T_i^{-1}(X)), \tag{9}$$

where $J_i^{-1}(X) = |dT_i^{-1}(X)/dX|$. The fixed point of this operator leads us to the stationary density. Therefore, we have

$$\rho(X) = \sum_{i=1}^{4} J_i^{-1}(X)\rho(T_i^{-1}(X)). \tag{10}$$

It is known that a functional relation of this type leads to solutions with multifractal characteristics.[7,19]

If we choose $S_i = T_i^{-1}$, this equation is of similar form to Eq. (4) used by Jaffard to define self-similar functions. To the best of our knowledge, Jaffard's theory of multifractal functions seems closest to the situation we have for the stationary density of coupled maps. However, as we shall discuss now, this available theory is still not adequate for our purpose as our multifractal spectra do not correspond to the results obtained here.

First, Jaffard's multifractal formalism for self-similar functions stipulates a nonzero minimum value for the Hölder exponent h given by the smallest value of $\log \lambda_i / \log \mu_i$ but in our case this smallest value is zero though none of our λ_is $(J_i^{-1}(X))$ are equal to one. Moreover, in the case of symmetric maps, *a priori*, one would not expect a multifractal structure as the values of λ_is and μ_i are the same for all i. More importantly, one would expect substantial variation in the multifractal spectrum with the change in the coupling constant ϵ and the skewness parameter (a and Δ) as that leads to the change in the values of the λ_is and μ_is. But that does not seem to happen. As a result, we come to the conclusion that this theory of multifractal functions is not able to capture at least the essential features of our findings.

It is necessary to understand the reasons of this failure to apply the existing theory. As it was mentioned before, there are several assumptions made in deriving the theory of multifractal spectra. Some of these assumptions are violated in our case. The first assumption is that $S_i(\Omega) \subset \Omega$. Figure 4 shows the sketches of $S_i(\Omega)$ for $i = 1, \ldots, 4$ for both the tent and the bit shift map. We can clearly see the portions going out of Ω. Also, there is an important assumption called OSC[19] which says that $S_i(\Omega) \cap S_j(\Omega) = \emptyset$. Again, Fig. 4 shows that there is a significant overlap between the images of different S_is applied to Ω. Another important assumption is that of isotropy which is not satisfied in the present models. We observe from Fig. 4 that the contraction ratios are different in the direction of the synchronization manifold and in the direction perpendicular to it. There is some work[27,28] to lift these restrictions but that too does not seem to be sufficient for our case.

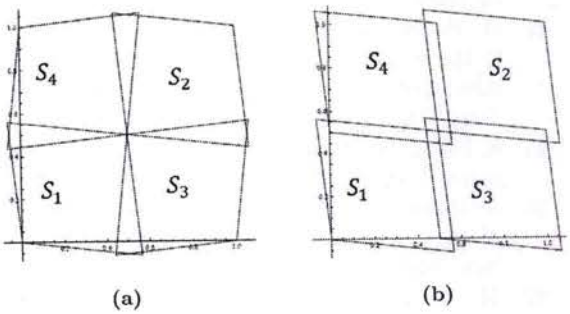

(a) (b)

Fig. 4 Sketches showing the overlap between different $T_i^{-1}(\Omega)$ for symmetric **(a)** tent map and **(b)** bit shift map.

It should also be pointed out that there have been some studies dealing with overlaps in the IFS especially by Hochman.[29] These have led to works on multifractal formalism of some IFS with overlaps.[30,31] However, Ref. 30 deals with a special class of one-dimensional measures, k-fold convolutions of Cantor-type measures, and Ref. 31 considers higher-dimensional systems but isotropic. Therefore, these results are not applicable here directly. They definitely give a direction for future exploration.

This suggests that a new mathematical theory which goes beyond these assumptions needs to be developed in order to account for the findings in this work.

4. CONCLUDING DISCUSSION

In the process of developing statistical understanding of coupled chaotic systems, we have uncovered a feature of the invariant density of two simple coupled chaotic maps. Our numerical results suggest that though the stationary density of the chosen individual map is usually a simple function, it becomes multifractal when two such maps are coupled. In spite of the fact that such systems have been studied extensively somehow this aspect was never explored. We have numerically studied symmetric and asymmetric tent maps as well as symmetric and asymmetric bit shift maps. It would have been natural to expect a systematic variation of the multifractal spectra with the coupling parameter or the asymmetry parameter, however, we find very robust spectra. This implies that there exists a universality class to which our examples belong. More investigations are needed to understand these observations including the extent of this universality class. As our preliminary numerical investigations have shown, the stationary density of the logistic map does not seem to lie in this class. We intend to analyze more complex maps with different couplings, different continuous systems and also non-identical coupled systems.

In order to rationalize the multifractal spectra that we observe, we formally arrived at a functional relation satisfied by the stationary density. By comparing the existing results for a similar functional relation, we find that the multifractal spectra we observe do not conform to those of the existing theory. Possibly, it is a result of violations of some assumptions in the theory, the important ones being those of overlap between different contractions of Ω and the anisotropy in these contractions. Also, the discontinuities at the boundaries introduced by the initial uniform distribution could also have a role to play. However, more analysis is needed to decide which of these reasons are crucial to the systems under study.

ACKNOWLEDGMENTS

We would like to acknowledge the financial help (EMR/2014/000255) from Science and Engineering Research Board (SERB), India. We are thankful to Herwig Wendt for the wavelet leaders code.

REFERENCES

1. A. Pikovsky, M. Rosenblum and J. Kurths, *Synchronization: A Universal Concept in Nonlinear Sciences* (Cambridge University Press, UK, 2003).
2. A. Politi and A. Torcini, Periodic orbits in coupled Hénon maps: Lyapunov and multifractal analysis, *Chaos* **2** (1992) 292–300.
3. A. Politi and G. P. Puccioni, Invariant measure in coupled maps, *Physica D* **58** (1992) 384–391.
4. B. B. Mandelbrot, *Fractal Geometry of Nature* (Freeman, USA, 1982).
5. J. Feder, *Fractals* (Plenum, USA, 1988).
6. M. F. Barnsley, *Fractals Everywhere* (Morgan Kaufmann, USA, 2000).
7. K. J. Falconer, *Fractal Geometry. Mathematical Foundations and Applications* (John Wiley, USA, 2003).
8. U. Frisch and G. Parisi, Fully developed turbulence and intermittency, in *Turbulence and Predictability of Geophysical Flows and Climate Dynamics*, Proceedings of the International School of Physics "Enrico Fermi" Course, Vol. LXXXVII (North-Holland, Amsterdam, 1985), pp. 71–88.
9. G. Paladin and A. Vulpiani, Anomalous scaling laws in multifractal objects, *Phys. Rep.* **156** (1987) 147–225.
10. A. Arneodo, B. Audit, B. Kestener and S. Roux, Wavelet-based multifractal analysis, *Scholarpedia* **3** (2008) 4103.
11. J. F. Muzy, E. Bacry and A. Arneodo, Wavelets and multifractal formalism for singular signals: Application to turbulence data, *Phys. Rev. Lett.* **67** (1991) 3515–3519.
12. J. F. Muzy, E. Bacry and A. Arneodo, The multifractal formalism revisited with wavelets, *Int. J. Bifur. Chaos* **4** (1994) 245–302.
13. E. Bacry, J. F. Muzy and A. Arneodo, Singularity spectrum of fractal signals from wavelet analysis: Exact results, *J. Statist. Phys.* **70** (1993) 635–674.
14. H. Wendt, P. Abry and S. Jaffard, Bootstrap for empirical multifractal analysis, *IEEE Signal Process. Mag.* **24** (2007) 38–48.
15. S. Jaffard, B. Lashermes and P. Abry, Wavelet leaders in multifractal analysis, in *Wavelet Analysis and Applications*, eds. T. Qian, M. I. Vai and Y. Xu (Birkhäuser Verlag, Basel, 2006), pp. 201–246.
16. E. Serrano and A. Figliola, Wavelet leaders: A new method to estimate the multifractal singularity spectra, *Physica A* **388** (2009) 2793–2805.
17. L. Olsen, A multifractal formalism, *Adv. Math.* **116**(1) (1995) 82–196.
18. I. Daubechies and J. C. Lagarias, On the thermodynamic formalism for multifractal functions, *Rev. Math. Phys.* **6** (1994) 1033–1070.
19. S. Jaffard, Multifractal formalism for functions part II: Self-similar functions, *SIAM J. Math. Anal.* **28** (1997) 971–998.
20. A. Ayache and S. Jaffard, Hölder exponents of arbitrary functions, *Rev. Mat. Iberoamericana* **26** (2010) 77–89.
21. J. Bezanson, A. Edelman, S. Karpinski and V. B. Shah, Julia: A fresh approach to numerical computing, *SIAM Rev.* **59** (2017) 65–98.
22. J. Jost and K. M. Kolwankar, Fractal stationary density in coupled maps, in *Fractals in Engineering: New Trends in Theory and Applications*, eds. J. Lévy-Vehel and E. Lutton (Springer, Berlin, 2005), pp. 57–64.
23. J. Jost and K. M. Kolwankar, Global analysis of synchronization in coupled maps, *Int. J. Bifur. Chaos* **16** (2006) 3695–3703.
24. M. Hasler and Y. L. Maistrenko, An introduction to the synchronization of chaotic systems: Coupled skew tent maps, *IEEE Trans. Circuits Systems I Fund. Theory Appl.* **44** (1997) 856–866.
25. H. Sakaguchi, Phase transitions in coupled Bernoulli maps, *Prog. Theor. Phys.* **80** (1988) 7–12.
26. A. Lasota and M. C. Mackey, *Chaos, Fractals, and Noise: Stochastic Aspects of Dynamics* (Springer, New York, 1994).
27. M. Ben Slimane, Multifractal formalism and anisotropic selfsimilar functions, *Math. Proc. Cambridge Philos. Soc.* **124** (1998) 329–363.

28. M. Ben Slimane, Multifractal formalism for self-similar functions associated to the n-scale dilation family, *Math. Proc. Cambridge Philos. Soc.* **136** (2004) 195–212.
29. M. Hochman, On self-similar sets with overlaps and inverse theorems for entropy, *Ann. Math.* **180**(2) (2014) 773–822.
30. P. Shmerkin, A modified multifractal formalism for a class of self-similar measures with overlap, *Asian J. Math.* **9** (2005) 323–348.
31. J. Barral and D.-J. Feng, On multifractal formalism for self-similar measures with overlaps, preprint (2020), arXiv:2002.02319.